PHYSICAL REVIEW B **83**, 054513 (2011)

Andreev reflection from noncentrosymmetric superconductors and Majorana bound-state generation in half-metallic ferromagnets

Mathias Duckheim and Piet W. Brouwer

Dahlem Center for Complex Quantum Systems and Institut für Physik, Freie Universität Berlin, D-14195 Berlin, Germany

(Received 26 November 2010; published 23 February 2011)

We study Andreev reflection at an interface between a half metal and a superconductor with spin-orbit interaction. While the absence of minority carriers in the half metal makes singlet Andreev reflection impossible, the spin-orbit interaction gives rise to triplet Andreev reflection (i.e., the reflection of a majority electron into a majority hole or vice versa). As an application of our calculation, we consider a thin half-metal film or wire laterally attached to a superconducting contact. If the half metal is disorder free, an excitation gap is opened that is proportional to the spin-orbit interaction strength in the superconductor. For electrons with energy below this gap a lateral half-metal–superconductor contact becomes a perfect triplet Andreev reflector. We show that the system supports localized Majorana end states in this limit.

DOI: 10.1103/PhysRevB.83.054513 PACS number(s): 74.45.+c, 74.78.Na, 75.70.Cn, 75.70.Tj

I. INTRODUCTION

Heterosystems with adjacent superconducting and ferromagnetic phases may show unconventional spin-triplet superconducting proximity effects even if the superconductor is of the conventional s-wave spin-singlet type.[1] Triplet correlations, even if they are weak, are important in ferromagnets, where the standard spin-singlet proximity effect is short ranged as a result of the exchange splitting.[2] In half metals singlet pairings are ruled out since, in a half metal, one spin species has zero density of states at the Fermi level so that the triplet version is the only possible form of the superconducting proximity effect. Microscopically, the superconducting proximity effect is mediated by Andreev reflection, the phase-coherent reflection of an electron into a hole or vice versa at the superconductor interface.[3] Triplet superconducting correlations then require a form of Andreev reflection that includes a spin flip.[4,5]

The triplet proximity effect has been considered first in ferromagnets (with a finite minority spin population), where the observation of long-range superconducting correlation effects[6–10] has been shown to be consistent with the existence of induced triplet correlations in the ferromagnet.[1,4] A number of mechanisms that give rise to the spin-flip Andreev reflection required for the triplet correlations, such as magnetic domain walls,[4] spin-orbit interaction,[11] and unconventional pairing correlations,[12] have been studied in hybrid ferromagnet-superconductor systems.

Long-range proximity effects have also been observed in half-metallic CrO_2–NbTiN[13] and CrO_2–MoGe[14] heterostructures. Because of the absence of minority carriers in the half metal it is concluded that the observed superconducting correlations must be of the triplet type.[13,15,16] However, in half metals the conditions for spin-flip Andreev reflection are more restrictive than in a ferromagnet. In particular, electron-hole symmetry and current conservation pose stronger restrictions on candidate mechanisms for spin-flip Andreev reflections than in ferromagnets:[17,18] If the interface is symmetric with respect to reflection in the surface normal, electron-hole symmetry and unitarity require the Andreev reflection amplitude $r_{he}(\varepsilon)$ to vanish at the Fermi energy $\varepsilon = 0$.[17] Thus, mechanisms that give rise to triplet Andreev reflection must either break electron-hole symmetry (i.e., take place away from the Fermi energy) or orbital symmetries. Mechanisms of the latter type are magnetization gradients in the half metal[18,19] or impurity scattering.[20]

In this article, we study spin-orbit interaction (SOI) in S as a possible mechanism giving rise to spin-flip Andreev reflection in a half metal (H). The presence of SOI is contingent on the breaking of inversion symmetry. Examples for systems with SOI in the normal state are surface states in Au,[21] semiconductor heterostructures, and two-dimensional (2D) electron gases in quantum wells with partially tunable SOI's.[22–24] Crystalline superconductors such as the noncentrosymmetric cuprates and heavy-fermion compounds such as $CePt_3Si$[25] and others[26] show SOI due to the absence of an inversion center in their crystal structure. These materials have received intense interest because they display unconventional superconducting (helical[27–29]) phases with mixed singlet and triplet pairing correlations,[26,30–33] magnetoelectric effects,[34,35] and an anisotropic spin susceptibility.[36,37] However, centrosymmetric superconducting materials also show SOI in surface or interfacial layers with inversion asymmetry. For instance, the breaking of inversion symmetry at a plane interface due to a change in the chemical potential gives rise to the Rashba SOI.[22,36]

In our calculation we assume a general model for the SOI that is linear in momentum and includes the Rashba SOI as a special case. In the first part of this article, we derive expressions for the electron-to-hole and hole-to-electron Andreev reflection amplitudes r_{he} and r_{eh} in a model Hamiltonian with parabolic dispersion in the half metal and in (the normal state of) the superconductor and to first order in the SOI. For our model Hamiltonian, which includes effects of a Fermi-velocity mismatch and a tunnel barrier at the half-metal–superconductor interface, we find that the Andreev reflection is such that the induced superconducting correlations in the vicinity of the superconducting interface are of even-frequency and complex p-wave type. This is a significant difference with other possible sources of triplet superconducting correlations in half metals, such as a nonuniform magnetization direction in the half metal, which also allow for odd-frequency s-wave proximity effects.

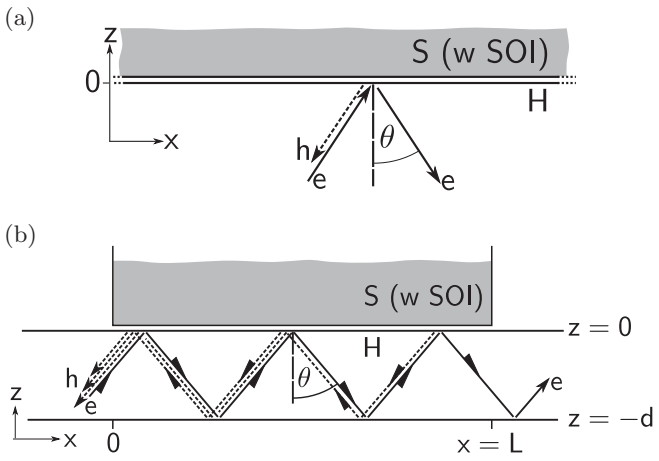

FIG. 1. (a) Interface between a half metal (H) and a superconductor (S). For a superconductor with spin-orbit scattering, normal reflection as well as triplet Andreev reflection—the reflection of a majority electron (e) into a majority hole (h)—take place at the HS interface. (b) A lateral contact between a half-metallic film or wire of thickness d and a superconductor. For a lateral contact, an effective Andreev reflection amplitude $r_{\rm he}^{\rm eff}$ for electrons moving toward the contact region can be defined, which describes the combined effect of multiple reflections at the H S interface.

Because Andreev reflection relies on the presence of SOI in the superconductor, the Andreev reflection probability $|r_{\rm he}|^2$ may be small depending on the strength of the SOI such that the induced superconducting correlations become weak. However, a fully developed proximity effect[38] can be achieved in a geometry in which multiple Andreev reflections occur. Examples of such geometries are a half-metallic film or wire in contact to a superconductor [shown schematically in Fig. 1(b)]. The latter example is closely related to recent proposals for the realization of Majorana fermions in a solid-state setting,[39–45] which, in turn, play an important role in proposals for topological quantum computation.[39,46] The second part of this article contains an investigation of multiple Andreev reflections in the film or wire geometry. We will show that the effect of multiple Andreev reflections can be combined into effective Andreev reflection amplitudes $r_{\rm he}^{\rm eff}$ and $r_{\rm eh}^{\rm eff}$. These effective amplitudes may have unit magnitude if sufficient reflection events contribute coherently them. We show that in this case localized Majorana states can be formed at the ends of a half-metal wire in contact to a superconductor with spin-orbit coupling. The investigation of the thin-film geometry is motivated by the recent experiments of Refs. 13 and 14.

In the present calculation we do not consider scattering from impurities in H or S. This does not seriously affect the first part of our calculation, which addresses the Andreev reflection amplitude for a single reflection off the HS interface, because the Andreev reflection amplitude is a local property of the interface. It is, however, a limitation for the second part of our calculation since the proximity effect induced by the multiple Andreev reflections is of the p-wave type, which is suppressed by impurity scattering. Thus the results derived in the second part of this article are valid only if the elastic mean free path in the half-metallic film or wire is sufficiently large.

The article is structured as follows. In Sec. II A we introduce the model Hamiltonian of the HS heterostructure and describe the calculation of the Andreev reflection amplitudes for a single reflection off a HS interface. As an application of our calculation, we calculate the subgap conductance of a half-metal–superconductor interface and the Josephson current in a superconductor–half-metal–superconductor junction in Sec. III. In Sec. IV we consider the geometry in which a thin half-metallic film is brought into electrical contact with a superconductor and derive the effective Andreev reflection amplitude $r_{\rm he}^{\rm eff}$ for this situation. Applications to the subgap conductance and Josephson effect in lateral HS and SHS junctions are then given in Sec. V. Finally, in Sec. VI, we consider a half-metallic wire placed in contact to a superconductor and relate our findings to predictions of the occurrence of Majorana fermions in such a system.

II. INTERFACE BETWEEN HALF METAL AND SUPERCONDUCTOR

A. Hamiltonian

We consider the interface between a half metal (H) and a superconductor (S) as shown in Fig. 1(a). Coordinates are chosen such that the superconductor and the half metal occupy the half spaces $z > 0$ and $z < 0$, respectively. Electron and hole excitations at excitation energy ε near the interface are described by the Bogoliubov-de–Gennes equation

$$\mathcal{H}\Psi = \varepsilon\Psi, \tag{1}$$

where $\Psi = (u_\uparrow, u_\downarrow, v_\uparrow, v_\downarrow)^{\rm T}$ is a four-component wave function with separate amplitudes for the particle/hole excitations (u, v) in the spin up/down bands $(\uparrow, \downarrow)$. The Bogoliubov-de–Gennes Hamiltonian $\mathcal{H}$ has the general form

$$\mathcal{H} = \begin{pmatrix} \hat{H}_0 & i\sigma_2\Delta(\mathbf{r}) \\ -i\sigma_2\Delta(\mathbf{r})^* & -\hat{H}_0^* \end{pmatrix}. \tag{2}$$

Here, the superconducting order parameter $\Delta(\mathbf{r}) = \Delta_0 e^{i\phi}\Theta(z)$, where $\Theta(z) = 1$ if $z > 0$ and 0 otherwise, and the σ_i are the Pauli matrices $i = 1, 2, 3$. We take the normal-state Hamiltonian H_0 to be of the form

$$\hat{H}_0 = \frac{\mathbf{p}^2}{2m} - \sum_{\sigma=\uparrow,\downarrow} \mu_\sigma(z)\hat{P}_\sigma + \hbar w\delta(z) + \hat{H}_{\rm SO}, \tag{3}$$

where m is the electron mass (taken to be the same in H and S)

$$\mu_\sigma(z) = \begin{cases} \mu_{{\rm H}\sigma} & \text{if} \quad z < 0, \\ \mu_{\rm S} & \text{if} \quad z > 0, \end{cases} \tag{4}$$

with the potentials $\mu_{\rm H\uparrow}$, $\mu_{\rm H\downarrow}$, and $\mu_{\rm S}$ representing the combined effect of the chemical potential and band offsets for the majority and minority electrons in the half metal and for the superconductor, respectively, and where w sets the strength of a δ-function potential barrier at the interface. The operators

$$\hat{P}_\uparrow = \tfrac{1}{2}(1 + \sigma_3), \quad \hat{P}_\downarrow = \tfrac{1}{2}(1 - \sigma_3), \tag{5}$$

project onto the majority and minority components, respectively. (The magnetization direction in H is taken as the spin quantization axis, which need not coincide with the z axis.) We will take the limit $\mu_{\mathrm{H}\downarrow} \to -\infty$, such that only the majority spin band is present in H. We further write

$$\mu_{\mathrm{H}\uparrow} = \frac{\hbar^2 k_{\mathrm{F,H}}^2}{2m}, \quad \mu_{\mathrm{S}} = \frac{\hbar^2 k_{\mathrm{F,S}}^2}{2m}, \tag{6}$$

where $k_{\mathrm{F,H}}$ and $k_{\mathrm{F,S}}$ are the Fermi wave numbers in H and S, respectively, and

$$\mu_{\mathrm{H}\downarrow} = -\frac{\hbar^2 \kappa^2}{2m}, \tag{7}$$

where κ is the minority wave function decay rate. The Fermi velocities are defined as

$$v_{\mathrm{F,H}} = \hbar k_{\mathrm{F,H}}/m, \quad v_{\mathrm{S,H}} = \hbar k_{\mathrm{S,H}}/m. \tag{8}$$

The step function model for the superconducting order parameter $\Delta(\mathbf{r})$ is justified for s-wave superconductors if the coupling to the half metal takes place via a tunnel barrier with transparency $\tau \ll 1$,[47] which corresponds to the requirement that $|w| \gg v_{\mathrm{F,H}}, v_{\mathrm{F,S}}$.

The operator $\hat{H}_{\mathrm{SO}}$ represents the effect of spin-orbit coupling. We consider the case that $\hat{H}_{\mathrm{SO}}$ is linear in the momentum $\mathbf{p}$ and that $\hat{H}_{\mathrm{SO}}$ is nonzero in S only[48]

$$\hat{H}_{\mathrm{SO}} = \frac{\hbar}{2}[\mathbf{p}\Theta(z) + \Theta(z)\mathbf{p}] \cdot \sum_{i=1}^{3} \mathbf{\Omega}_i \sigma_i, \tag{9}$$

where we denote $\mathbf{\Omega}_i = (\Omega_{i,x}, \Omega_{i,y}, \Omega_{i,z})^T$. Such a SOI may originate from the breaking of inversion symmetry by the crystal structure of S or due to an inversion asymmetry of the HS heterosystem. We assume that the spin-orbit interaction is weak, $\hbar|\mathbf{\Omega}(\mathbf{k}_{\mathrm{F,S}})| \ll v_{\mathrm{F,H}}, v_{\mathrm{S,H}}$, so that it can be captured by treating $\hat{H}_{\mathrm{SO}}$ to first order in perturbation theory.

In addition to the spin-singlet order parameter contained in Eq. (2), the presence of SOI generally allows for a triplet contribution to the order parameter, which is of the form $\Delta(\mathbf{p}) = \sum_{i=1}^{3} \Delta_i(\mathbf{p})\sigma_i$. Because of the Pauli principle, these triplet components are odd in momentum, $\Delta_i(-\mathbf{p}) = -\Delta_i(\mathbf{p})$. Such a triplet contribution is absent if the pairing interaction is isotropic,[49] but it may be present if the pairing interaction is anisotropic.[36] In Appendix B we include triplet pairings in the model and give the results for the Andreev reflection amplitudes. The spin-orbit interaction does not lead to a modification of the magnitude of the spin-singlet order parameter to first order in $\hat{H}_{\mathrm{SO}}$.

B. Andreev reflection amplitudes

We now calculate the Andreev reflection amplitudes for of the interface between H and S using the Blonder-Tinkham-Klapwijk formalism.[50] At the HS interface triplet, Andreev reflection occurs because quasiparticles incident on the interface from H penetrate the superconductor over a finite length before being reflected. Due to the SOI, spin is not a good quantum number in S, which makes spin-flip reflection possible. The Andreev reflection amplitudes are found by matching eigenfunctions of $\mathcal{H}$ in H and S to linear order in the SOI. (An alternative method, using perturbation theory in the SOI Hamiltonian, will be described at the end of this section.) The matching conditions, continuity and conservation of particle flux, hold for plane-wave eigenstates in the immediate proximity of the interface on length scales of the Fermi wavelength. Thus, the S matrix of the interface is a local property and will not be changed by weak disorder.

The starting point of the matching procedure are expressions for the general solutions of the Bogoliubov-de Gennes equation in H and S, near the HS interface. Because of translation symmetry along the interface, we can consider plane-wave solutions with wave numbers k_x and k_y in the x and y directions parallel to the interface. In H, one then finds six linearly independent solutions, which we label $\Psi_{\mathrm{e},\uparrow,\pm}$, $\Psi_{\mathrm{h},\uparrow,\pm}$, $\Psi_{\mathrm{e},\downarrow}$, and $\Psi_{\mathrm{h},\downarrow}$,

$$\Psi_{\mathrm{e},\uparrow,\pm}(\mathbf{r}) = \frac{e^{\pm i k_z(+\varepsilon)z + i k_x x + i k_y y}}{\sqrt{v_z(\varepsilon)}}(1,0,0,0)^{\mathrm{T}}, \tag{10}$$

$$\Psi_{\mathrm{h},\uparrow,\pm}(\mathbf{r}) = \frac{e^{\mp i k_z(-\varepsilon)z + i k_x x + i k_y y}}{\sqrt{v_z(-\varepsilon)}}(0,0,1,0)^{\mathrm{T}}, \tag{11}$$

$$\Psi_{\mathrm{e},\downarrow}(\mathbf{r}) = e^{\kappa_z(+\varepsilon)z + i k_x x + i k_y y}(0,1,0,0)^{\mathrm{T}}, \tag{12}$$

$$\Psi_{\mathrm{h},\downarrow}(\mathbf{r})\text{`} = e^{\kappa_z(-\varepsilon)z + i k_x x + i k_y y}(0,0,0,1)^{\mathrm{T}}, \tag{13}$$

where $k_z(\varepsilon)$ and $\kappa_z(\varepsilon)$ are the positive solutions of

$$\begin{aligned} k_z(\varepsilon)^2 &= k_{\mathrm{F,H}}^2 - k_{||}^2 + 2m\varepsilon/\hbar^2, \\ \kappa_z(\varepsilon)^2 &= \kappa^2 + k_{||}^2 - 2m\varepsilon/\hbar^2, \end{aligned} \tag{14}$$

and

$$\mathbf{k}_{\parallel} = (k_x, k_y, 0)^{\mathrm{T}}, \tag{15}$$

is the momentum parallel to the interface and

$$v_z(\varepsilon) = \hbar k_z(\varepsilon)/m. \tag{16}$$

The states labeled with $+$ and $-$ are majority states moving toward or away from the interface, respectively. They are normalized to unit flux. The states labeled with $\downarrow$ are minority states that decay into the half metal. They appear in intermediate stages of the calculation only and their normalization is not important.

Only the spin-orbit interaction terms proportional to $\mathbf{\Omega}_1$ and $\mathbf{\Omega}_2$ give rise to spin flips in the superconductor. For a calculation of Andreev reflection amplitudes linear in the SOI, it is then sufficient to set $\mathbf{\Omega}_3 = 0$, which significantly simplifies the form of the solutions of the Bogoliubov-de–Gennes equation in S. In S, one then finds four linearly independent solutions $\Psi_{s,t}$ of the Bogoliubov-de–Gennes equation $t, s = \pm 1$, which read

$$\Psi_{s,t}(\mathbf{r}) = \frac{1}{2}\begin{pmatrix} 1 \\ e^{i\gamma_{s,t}} \\ e^{-i\phi - is\eta + i\gamma_{s,t}} \\ e^{-i\phi - is\eta} \end{pmatrix} e^{i q_{s,t} z + i k_x x + i k_y y}, \tag{17}$$

where

$$\eta = \arccos(\varepsilon/\Delta_0), \tag{18}$$

$$q_{s,t} = t\sqrt{k_{\mathrm{F,S}}^2 - k_{||}^2 + 2itm\sqrt{\Delta_0^2 - \varepsilon^2}} - mst\Omega_{s,t}, \tag{19}$$

and $\gamma_{s,t}$ and $\Omega_{s,t}$ are defined such that

$$(\mathbf{\Omega}_1 + i\mathbf{\Omega}_2)\cdot\mathbf{q} = \Omega_{s,t} q e^{i\gamma_{s,t}}, \tag{20}$$

with $\mathbf{q} = (k_x, k_y, q_{s,t})^{\mathrm{T}}$.

A complete solution $\Psi(\mathbf{r})$ of the Bogoliubov-de–Gennes equation consists of a linear combination of the six special solutions (10)–(13) in H for $z < 0$ and a linear combination of the four special solutions (17) in S, with the boundary conditions

$$\Psi(\mathbf{r})|_{z=0^-} = \Psi(\mathbf{r})|_{z=0^+} \tag{21}$$

$$\left.\frac{\partial\Psi(\mathbf{r})}{\partial z}\right|_{z=0^-} = \left.\frac{\partial\Psi(\mathbf{r})}{\partial z}\right|_{z=0^+} + m\left(i\sum_{j=1}^{3}\Omega_{j,z}\sigma_j + \frac{2w}{\hbar}\right)\Psi(\mathbf{r})\Big|_{z=0^+} \tag{22}$$

at the interface $z = 0$. Since $\Psi(\mathbf{r})$ is a four-component spinor, the boundary conditions provide eight linear relations between the coefficients of the ten basis functions. The Andreev amplitude r_{he} is then defined as the coefficient of $\Psi_{\mathrm{h},\uparrow,-}$ if the coefficients of the two incoming wave solutions $\Psi_{\mathrm{e},\uparrow,+}$ and $\Psi_{\mathrm{h},\uparrow,+}$ are chosen to be 1 and 0, respectively. Analogously, the Andreev amplitude r_{eh} is defined as the coefficient of $\Psi_{\mathrm{e},\uparrow,-}$ if the coefficients of $\Psi_{\mathrm{e},\uparrow,+}$ and $\Psi_{\mathrm{h},\uparrow,+}$ are chosen to be 0 and 1, respectively. To lowest order in the SOI and to lowest order in the normal-state transmission $\tau(\theta)$ of the HS interface, we find that

$$r_{\mathrm{he}}(\mathbf{k}_\parallel,\varepsilon) = \frac{-im\tau(\theta)e^{-i\phi}(\mathbf{\Omega}_1 + i\mathbf{\Omega}_2)\cdot\mathbf{k}_\parallel\Delta_0}{2\left(k_{\mathrm{F,S}}^2 - k_{\mathrm{F,H}}^2\sin^2\theta\right)\sqrt{\Delta_0^2 - \varepsilon^2}}, \tag{23}$$

and

$$\begin{aligned} r_{\mathrm{eh}}(\mathbf{k}_\parallel,\varepsilon) &= r_{\mathrm{he}}(-\mathbf{k}_\parallel, -\varepsilon)^* \\ &= \frac{-im\tau(\theta)e^{i\phi}(\mathbf{\Omega}_1 - i\mathbf{\Omega}_2)\cdot\mathbf{k}_\parallel\Delta_0}{2\left(k_{\mathrm{F,S}}^2 - k_{\mathrm{F,H}}^2\sin^2\theta\right)\sqrt{\Delta_0^2 - \varepsilon^2}}. \end{aligned} \tag{24}$$

Here $\theta = \arcsin(|\mathbf{k}_\parallel|/k_{\mathrm{F,H}})$ is the angle between the incident momentum and the interface normal, see Fig. 1, and

$$\tau(\theta)^2 = \frac{v_{\mathrm{F,H}}^2\cos^2\theta\left(v_{\mathrm{F,S}}^2 - v_{\mathrm{F,H}}^2\sin^2\theta\right)}{w^4} + \mathcal{O}\left(\frac{1}{w^6}\right). \tag{25}$$

Equation (23) has been simplified using the "Andreev approximation," which amounts to neglecting corrections of order $\mathcal{O}(\varepsilon/E_{\mathrm{F,S}}, \Delta_0/E_{\mathrm{F,S}})$. (This approximation is uniformly valid for all angles if $k_{\mathrm{F,S}} > k_{\mathrm{F,H}}$. If $k_{\mathrm{F,S}} \leqslant k_{\mathrm{F,H}}$ there is a small range of angles for which the approximation fails.)

The divergence for $\varepsilon \to \pm\Delta$ in Eqs. (23) and (24) is a consequence of the expansion in the normal-state transmission coefficient τ of the HS interface and has to be cutoff for $1 - (\varepsilon/\Delta)^2 \lesssim \tau^2$. This means that the immediate vicinity of $\pm\Delta$ has to be excluded from the region of validity of Eqs. (23) and (24) so that these equations are valid for $1 - (\varepsilon/\Delta)^2 \gg \tau^2$ only. The same condition will be required for the validity of Eq. (26) and for expressions that are derived from these equations. (We note that similar restrictions also apply to an expansion in the transmission coefficient for a normal-metal–superconductor interface, see, e.g., Ref. 50.)

For completeness, we also give the results for the normal reflection amplitudes r_{ee} and r_{hh} of the HS interface consistent with the assumptions of our calculation

$$r_{\mathrm{ee}}(\mathbf{k}_\parallel,\varepsilon) = -1 + i\sqrt{\frac{\tau(\theta)k_{\mathrm{F,H}}\cos\theta}{\sqrt{k_{\mathrm{F,S}}^2 - k_{\mathrm{F,H}}^2\sin^2\theta}}} + \frac{\tau(\theta)}{2}\left(\frac{k_{\mathrm{F,H}}\cos\theta}{\sqrt{k_{\mathrm{F,S}}^2 - k_{\mathrm{F,H}}^2\sin^2\theta}} - \frac{i\varepsilon}{\sqrt{\Delta_0^2 - \varepsilon^2}}\right), \tag{26}$$

$$r_{\mathrm{hh}}(\mathbf{k}_\parallel,\varepsilon) = r_{\mathrm{ee}}^*(-\mathbf{k}_\parallel, -\varepsilon). \tag{27}$$

Alternatively, Eqs. (23) and (24) can be obtained from a calculation of the first-order perturbation theory correction to the scattering matrix of the HS interface without spin-orbit interaction. This calculation is outlined in the Appendix (see Ref. 18 for more details).

Equations (23) and (24) are the two central results of the first part of this article. Although the Andreev reflection amplitudes have been derived for a specific model Hamiltonian and in the limit of a tunneling interface, we believe that the symmetry properties of r_{he} and r_{eh} (r_{he} and r_{eh} are *odd* in $\mathbf{k}_\parallel$ and *even* in ε) persist in a more general calculation, as long as the SOI is linear in momentum. We have verified this statement for the cases that a finite minority-wave function decay rate κ is included in the calculation, that the spin-orbit interaction extends only a finite distance into the superconductor, and that higher-order terms in the interface transmission $\tau(\theta)$ are included (see Appendix A for details).

The antisymmetry of r_{he} and r_{eh} as a function of $\mathbf{k}_\parallel$ implies that the Andreev reflection amplitudes r_{he} and r_{eh} contain only four elements $\Omega_{1,x}$, $\Omega_{1,y}$, $\Omega_{2,x}$, and $\Omega_{2,y}$ of the spin-orbit coupling matrix. We had already discussed, that the three elements $\Omega_{3,x}$, $\Omega_{3,y}$, and $\Omega_{3,z}$ that describe the coupling between the spin component parallel to the magnetization direction and the orbital motion of the electrons do not give rise to spin flips and hence do not contribute to the Andreev reflection amplitude. Equations (23) and (24) show that the same is true for the elements $\Omega_{1,z}$, $\Omega_{2,z}$, and $\Omega_{3,z}$ of the spin-orbit coupling matrix that couple the electron spin to the orbital motion perpendicular to the interface and thus provide a spin-flip mechanism that is symmetric in $\mathbf{k}_\parallel$. For zero excitation energy ε, this observation can be understood from the general symmetry considerations of Ref. 18, which stated that $r_{\mathrm{he}}(\mathbf{k}_\parallel, 0) = 0$ if r_{he} is a symmetric function of $\mathbf{k}_\parallel$. That this remains true for nonzero ε is special to the case of spin-orbit coupling as a source of spin-flip scattering and requires the explicit calculation of this section.

There is a direct relation between the Andreev reflection amplitudes r_{he} and r_{eh} and the anomalous Green function $f(\mathbf{k}, i\omega)$,[18]

$$f(\mathbf{k},i\omega) \propto \begin{cases} \Theta(-k_z)r_{\mathrm{eh}}(\mathbf{k}_\parallel,i\omega) & \text{if } \omega > 0, \\ -\Theta(k_z)r_{\mathrm{he}}(\mathbf{k}_\parallel, -i\omega)^* & \text{if } \omega < 0, \end{cases} \tag{28}$$

up to a prefactor that is not important for the identification of the symmetries of f. Since $r_{\mathrm{he}}(\mathbf{k}_\parallel, -i\omega)^* = -r_{\mathrm{eh}}(\mathbf{k}_\parallel, i\omega)$ in the present case, see Eq. (24), one concludes that the induced

superconducting correlations in H are odd in momentum [i.e., predominantly of (complex) p-wave type] and even in frequency.

III. APPLICATIONS: SUBGAP CONDUCTANCE AND JOSEPHSON CURRENT

As an application, we now calculate the subgap conductance of an HS junction and the Josephson current of a superconductor–half-metal–superconductor (SHS) junction.

A. Subgap conductance

We assume the interface to have lateral dimensions $W_x \times W_y$ and impose periodic boundary conditions in these directions. This leads to a quantization of the transverse modes with wave numbers $k_{n_x} = 2\pi n_x/W_x$ and $k_{n_y} = 2\pi n_y/W_y$, n_x and n_y integers. At zero temperature, the differential conductance $G = dI/dV$ can be calculated in terms of the Andreev reflection amplitudes $r_{\rm he}$. Replacing the summation over modes by an integral, we find[50,51]

$$G(V) = \tfrac{2e^2}{h}\mathrm{Tr}|r_{\rm he}(\mathbf{k}_\parallel, eV)|^2, \tag{29}$$

where $\mathrm{Tr}\{\ldots\} = W_x W_y/(4\pi^2)\int_{k_\parallel<k_{\rm F,H}} d\mathbf{k}_\parallel\{\ldots\}$ is the trace over transverse mode $\mathbf{k}_\parallel$. The factor of 2 is due to the doubling of the transferred charge by conversion of an electron into a hole upon Andreev reflection.

Substituting Eq. (23) for the Andreev reflection amplitude $r_{\rm he}$ and performing the integrations over k_x and k_y, we then find

$$G(V) = \frac{e^2}{h}\frac{3N}{8}\frac{\langle\tau^2\rangle_\theta \Delta_0^2}{\Delta_0^2 - (eV)^2} \times \frac{\hbar^2\left(\Omega_{1,x}^2 + \Omega_{2,x}^2 + \Omega_{1,y}^2 + \Omega_{2,y}^2\right)}{v_{\rm F,H}^2}, \tag{30}$$

where $N = k_{\rm F,H}^2 W_x W_y/4\pi$ is the number of propagating channels in H and

$$\langle\ldots\rangle_\theta = 2\int_0^{\pi/2} d\theta \ldots \sin\theta\cos\theta, \tag{31}$$

denotes an average over the angle of incidence θ.

B. Josephson current

For the Josephson effect, we consider a half-metallic junction of length $L_{\rm j}$ separating two superconducting contacts. Again, we take the junction to have lateral dimensions $W_x \times W_y$ and impose periodic boundary conditions in the x and y directions. Taking periodic boundary conditions is justified if the lateral dimensions $W_{x,y} \gg L_{\rm j}$, see Fig. 2(a). We further take both HS interfaces to have the same normal-state transmission $\tau(\theta)$, take the same spin-orbit interaction Hamiltonian $\hat{H}_{\rm SO}$ in both superconductors, and neglect impurity scattering in the half-metallic junction.

The Josephson current can be found from the density of states in the junction which, in turn, may be expressed in terms of the scattering matrices of the HS interfaces (see Ref. 52 and 53 for details). In the absence of impurity scattering, the contributions to the Josephson current from

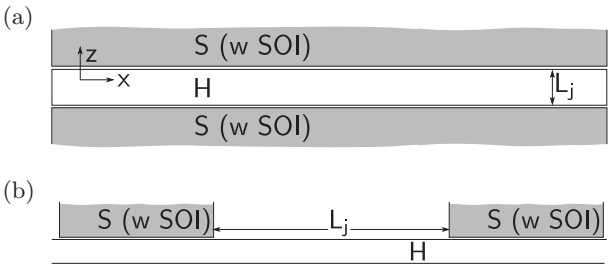

FIG. 2. (a) Serial and (b) a lateral superconductor–half-metal–superconductor (SHS) junction.

different transverse wave vectors $\mathbf{k}_\parallel$ add up, and one finds that the Josephson current at temperature T is given by the expression

$$I = -\frac{2ek_{\rm B}T}{\hbar}\frac{d}{d\phi}\sum_{n=0}^{\infty} \times \mathrm{Tr}\{\ln\det[1 - \mathcal{R}(\mathbf{k}_\parallel, i\omega_n)\mathcal{R}'(\mathbf{k}_\parallel, i\omega_n)]\}, \tag{32}$$

where $\omega_n = (2n+1)\pi k_{\rm B}T$ is the Matsubara frequency, $\mathcal{R}$ is a 2×2 reflection matrix containing reflection and transmission amplitudes for the first HS interface,

$$\mathcal{R}(\mathbf{k}_\parallel, i\omega_n) = \begin{pmatrix} e^{ik_z(i\omega_n)L_{\rm j}} & 0 \\ 0 & e^{-ik_z(-i\omega_n)L_{\rm j}} \end{pmatrix} \times \begin{pmatrix} r_{\rm ee}(\mathbf{k}_\parallel, i\omega_n) & r_{\rm eh}(\mathbf{k}_\parallel, i\omega_n) \\ r_{\rm he}(\mathbf{k}_\parallel, i\omega_n) & r_{\rm hh}(\mathbf{k}_\parallel, i\omega_n) \end{pmatrix}, \tag{33}$$

with $k_z(\varepsilon)$ is given in Eq. (14) and the reflection amplitudes given by Eqs. (23)–(27) above, and $\mathcal{R}'(\mathbf{k}_\parallel, i\omega_n)$ is a similar matrix describing Andreev reflection at the second HS interface. Specifically, in the serial geometry in Fig. 2(a), $\mathcal{R}'(\mathbf{k}_\parallel, i\omega_n) = \mathcal{R}(\mathbf{k}_\parallel, i\omega_n)|_{\phi=0}$ with the phase of the order parameter set to zero.

Closed-form expressions for the Josephson current I can be obtained in limiting cases only. In the limit of a "long" junction, $L_{\rm j} \gg \xi$, where $\xi = \hbar v_{\rm F,H}/\Delta_0$ is the superconducting coherence length, and for high temperatures $k_{\rm B}TL_{\rm j}/\hbar v_{\rm F,H} \gg 1$ one finds

$$eI = \frac{2e^2}{h} 8\pi k_{\rm B}T\sin(\phi)\mathrm{Tr}\left\{|r_{\rm he}(\mathbf{k}_\parallel, i\omega_0)|^2_{\phi=0}\, e^{2\omega_0 L/v_z(0)}\right\}. \tag{34}$$

Performing the integration over the transverse momentum $\mathbf{k}_\parallel$ for the parabolic dispersion of our model Hamiltonian then gives the result

$$eI = \frac{2\pi k_{\rm B}T\sin\phi}{3} G(0) f(2\pi k_{\rm B}TL_{\rm j}/\hbar v_{\rm F,H}), \tag{35}$$

where $G(0)$ is the zero-bias conductance of a single HS interface, see Eq. (30), and

$$f(x) = e^{-x}(6 - 10x - x^2 + x^3) + x^2(x^2 - 12)\mathrm{Ei}(-x) \approx 48e^{-x}/x^2 \quad \text{for } x \gg 1, \tag{36}$$

with the exponential integral $\mathrm{Ei}(x) = -\int_{-x}^{\infty} dt e^{-t}/t$.

In the opposite limit of zero temperature, the expression for the Josephson current in a long junction ($L_{\rm j} \gg \xi$)

becomes

$$I = \frac{2e\sin\phi}{\hbar}\int_0^\infty d\omega \times \mathrm{Tr}\left\{\frac{|r_{\rm he}|^2}{\cosh\frac{2\omega L_{\rm j}}{v_z} - \mathrm{Re}\left[r_{\rm ee}^2 e^{2ik_z(0)L}\right] + |r_{\rm he}|^2\cos\phi}\right\}. \quad (37)$$

Normal reflection with amplitude $r_{\rm ee}$ at the two HS interfaces gives rise to terms in Eq. (37) that oscillate with the junction length $L_{\rm j}$. These oscillations disappear once the trace over transverse modes is taken since $k_z(0)L_{\rm j} \gg 1$ for long junctions. The remaining nonoscillatory contribution to the supercurrent $\bar{I}$ can then be calculated by taking the average $\bar{I} = (2\pi)^{-1}\int_0^{2\pi} d\chi\, I(\chi)$, where $I(\chi)$ is obtained from Eq. (37) by the replacement $2ik_z(0)L_{\rm j} \to \chi$. One thus obtains

$$I = \frac{e\sin\phi}{2L_{\rm j}}\mathrm{Tr}\left\{v_z|r_{\rm he}|^2\log\left[\frac{16\sin^2(\phi/2)}{|r_{\rm he}|^2\sin^2\phi}\right]\right\}. \quad (38)$$

The remaining trace over modes can be performed to logarithmic accuracy by neglecting the dependence of the argument of the logarithm on $\mathbf{k}_\parallel$. This amounts to the replacement $|r_{\rm he}|^2 \to \langle|r_{\rm he}|^2\rangle_\theta = hG(0)/2e^2N$ in the argument of the logarithm. One then obtains

$$eI = \frac{4\pi\hbar v_{\rm F}}{15L_{\rm j}}G(0)\sin\phi\log\left[\frac{32e^2N\sin^2(\phi/2)}{hG(0)\sin^2\phi}\right], \quad (39)$$

up to corrections of order $G(0)\hbar v_{\rm F}/L_{\rm j}$, but without the large logarithm $\log(e^2N/G(0)h$. The small corrections to the approximately sinusoidal phase dependence of the supercurrent in Eq. (39) originate from scattering processes with multiple normal reflections at the HS interfaces.

IV. LATERAL GEOMETRY

An experimentally relevant situation[13,14] is the lateral geometry where the superconducting contact is attached laterally to a thin H film. This situation is shown in Fig. 1(b). In comparison to the serial contact considered in the previous section, a lateral contact has a significantly larger contact area per unit cross section of H. Multiple reflections occur at the HS interface because quasiparticles are repeatedly reflected backward from the lower film boundary toward the interface. In the absence of impurity scattering in the half-metallic film, the coherent addition of these multiple Andreev reflections leads to a significant enhancement of the Andreev reflection probability for a quasiparticle incident on the lateral contact from the left [in Fig. 1(b)], as we now show.

We choose coordinates such that the half metal occupies the region between $z = 0$ and $z = -d$ and the superconductor occupies the region $x > 0$, $z > 0$, see Fig. 1(b). We take periodic boundary conditions in the y direction, with system size W_y. For the half metal, we take hard-wall (Dirichlet) boundary conditions at $z = -d$ for all x, and at $z = 0$ for $x < 0$. The thickness d of the half-metallic film is taken to be much smaller than the superconducting coherence length $\xi = \hbar v_{\rm F,H}/\Delta_0$. As before, we take the HS interface to be a tunneling interface with a transmission probability $\tau(\theta) \ll 1$.

The goal of our calculation is to find the amplitude $r_{\rm he}^{\rm eff}$ that a right-moving electron-like quasiparticle approaching the contact from the left is Andreev reflected into a left-moving hole-like quasiparticle, as well as the amplitude $r_{\rm eh}^{\rm eff}$ for the process that a hole-like quasiparticle is Andreev reflected as an electron-like quasiparticle. The calculation proceeds in three steps. First, we construct scattering states in the absence of spin-orbit interaction. Second, we account for the effect of spin-orbit interaction in a superconducting region of length $d, \delta L \ll \xi$ using perturbation theory. Finally, we combine Andreev reflections from different segments and compute the Andreev reflection amplitudes $r_{\rm he}^{\rm eff}$ and $r_{\rm eh}^{\rm eff}$.

A. Scattering states in the absence of SOI

Because of translation symmetry in the y direction, the scattering states can be chosen as plane waves in the y direction with wave number k_y, which takes discrete values only because of the periodic boundary conditions in the y direction. We first construct scattering states for $x < 0$. There, because of the hard-wall boundary conditions at $z = 0$ and $z = -d$, the z dependence can be chosen proportional to $\sin(k_z z)$, where $k_z = n\pi/d, n = 1, 2, \ldots$, is discrete as well. For each discrete value of the transverse momenta $\mathbf{k}_\perp = (0, k_y, k_z)^{\rm T}$ one then has four scattering states that we label $\Phi_{{\rm e},\mathbf{k}_\perp\pm}$ and $\Phi_{{\rm h},\mathbf{k}_\perp,\pm}$,

$$\Phi_{{\rm e},\mathbf{k}_\perp,\pm}(\mathbf{r}) = \frac{2e^{\pm ik_x(\varepsilon)x + ik_y y}\sin(k_z z)}{\sqrt{v_x d W_y}}\begin{pmatrix}1\\0\\0\\0\end{pmatrix}, \quad (40)$$

$$\Phi_{{\rm h},\mathbf{k}_\perp,\pm}(\mathbf{r}) = \frac{2e^{\mp ik_x(-\varepsilon)x + ik_y y}\sin(k_z z)}{\sqrt{v_x d W_y}}\begin{pmatrix}0\\0\\1\\0\end{pmatrix}, \quad (41)$$

where $k_x(\varepsilon)$ is the positive solution of

$$k_x(\varepsilon)^2 = k_{\rm F,H}^2 - k_y^2 - k_z^2 + \frac{2m\varepsilon}{\hbar^2}, \quad (42)$$

and

$$v_x = \hbar k_x/m. \quad (43)$$

The scattering states labeled "+" represent quasiparticle states moving to the left; the states labeled "−" represent quasiparticle states moving to the right. All scattering states are normalized to unit flux.

In the region $x > 0$, the scattering states differ from those given above because of the finite tunnel coupling to the superconductor. In particular, the scattering states acquire a finite weight inside the superconductor. In the tunneling limit $\tau \ll 1$, this weight is small and the majority component of the scattering states inside the half metal remains well approximated by Eqs. (40) and (41). The exact expressions for the full scattering state in the region $x > 0$ are cumbersome, and we refer to Ref. 18 where the detailed expressions can be found.

The "turning on" of the tunnel coupling to the superconductor at $x = 0$ gives rise to a small amount of normal reflection, but it does not cause Andreev reflection. We neglect this normal reflection at $x = 0$ in the remainder of this section.

B. Andreev reflection from a superconducting segment of length δL

The presence of spin-orbit coupling in the superconductor gives rise to Andreev reflection at the HS interface, as we have seen in Sec. III. In the second step of our calculation, we compute the effective Andreev reflection amplitude for a superconducting segment of size $0 < x < \delta L$. We choose the length δL of the superconducting segment such that $d, \delta L \ll \xi$. The inequality $d \ll \xi$, together with translation symmetry in the y direction, ensure that the Andreev reflection amplitude is diagonal in k_y and k_z. The inequality $\delta L \ll \xi$ gives $|k_x(\varepsilon) - k_x(-\varepsilon)|\delta L \ll 1$ for excitation energies up to Δ_0. This, in turn, leads to Andreev reflection amplitudes proportional to δL, which we write as $\rho_{\rm he}(\mathbf{k}_\perp,\varepsilon)\delta L$ and $\rho_{\rm eh}(\mathbf{k}_\perp,\varepsilon)\delta L$, for electron-to-hole and hole-to-electron reflection, respectively.

Calculating the Andreev amplitudes for the segment $0 < x < \delta L$ in first-order perturbation theory in the spin-orbit interaction gives

$$\begin{aligned}\rho_{\rm he}(\mathbf{k}_\perp,\varepsilon)\delta L &= -i\langle \Phi_{{\rm h},\mathbf{k}_\perp,-}|\delta\mathcal{H}_{\rm SO}|\Phi_{{\rm e},\mathbf{k}_\perp,+}\rangle,\\ \rho_{\rm eh}(\mathbf{k}_\perp,\varepsilon)\delta L &= -i\langle \Phi_{{\rm e},\mathbf{k}_\perp,-}|\delta\mathcal{H}_{\rm SO}|\Phi_{{\rm h},\mathbf{k}_\perp,+}\rangle,\end{aligned} \tag{44}$$

where $\delta\mathcal{H}_{\rm SO}$ is the 4×4 matrix Hamiltonian representing the projection of the spin-orbit interaction Hamiltonian onto the segment $0 < x < \delta L$,

$$\delta\mathcal{H}_{\rm SO} = \tfrac{1}{2}\{P_{\delta L}(x),\mathcal{H}_{\rm SO}\}, \tag{45}$$

$$\mathcal{H}_{\rm SO} = \begin{pmatrix}\hat{H}_{\rm SO} & 0\\ 0 & -\hat{H}^*_{\rm SO}\end{pmatrix}, \tag{46}$$

with $P_{\delta L}(x) = 1$ for $0 < x < \delta L$ and 0 otherwise. Evaluating the matrix element in the limit $d \ll \delta L \ll \xi$ then gives

$$\rho_{\rm he}(\mathbf{k}_\perp,\varepsilon) = r_{\rm he}(\mathbf{k}_\parallel,\varepsilon)\frac{k_z}{2dk_x}, \tag{47}$$

where $\mathbf{k}_\parallel = (k_x(0),k_y,0)^{\rm T}$. Equation (47) has the simple interpretation as the Andreev reflection amplitude for a single reflection at the HS interface, multiplied by the number of bounces at the HS interface per unit length.[18,19] Similarly, one finds that

$$\rho_{\rm eh}(\mathbf{k}_\perp,\varepsilon) = r_{\rm eh}(\mathbf{k}'_\parallel,\varepsilon)\frac{k_z}{2dk_x}, \tag{48}$$

where $\mathbf{k}'_\parallel = (-k_x(0),k_y,0)^{\rm T}$.

In the same way, one also calculates Andreev reflection amplitudes $\rho_{\rm he}(\mathbf{k}_\perp,\varepsilon)'\delta L$ and $\rho_{\rm he}(\mathbf{k}_\perp,\varepsilon)'\delta L$ for quasiparticles incident on the segment $0 < x < \delta L$ from the right. These are

$$\rho_{\rm he}(\mathbf{k}_\perp,\varepsilon)' = r_{\rm he}(\mathbf{k}'_\parallel,\varepsilon)\frac{k_z}{2dk_x}, \tag{49}$$

$$\rho_{\rm eh}(\mathbf{k}_\perp,\varepsilon)' = r_{\rm eh}(\mathbf{k}_\parallel,\varepsilon)\frac{k_z}{2dk_x}. \tag{50}$$

C. Effective Andreev reflection amplitudes for the lateral contact

In the final part of the calculation, we consider a superconducting contact of finite length $0 < x < L$. To keep the notation simple, we omit the arguments $\mathbf{k}_\perp$ and ε in the intermediate results.

Upon comparing contacts of length L and $L+\delta L$, one finds that

$$\begin{aligned}r^{\rm eff}_{\rm he}(L+\delta L) = r^{\rm eff}_{\rm he}(L)e^{i(k_x(\varepsilon)-k_x(-\varepsilon))\delta L}\\ +\left[\rho_{\rm he}+\rho'_{\rm eh}r^{\rm eff}_{\rm he}(L)^2\right]\delta L + \mathcal{O}(\delta L)^2.\end{aligned} \tag{51}$$

Making use of the relations

$$\rho'_{\rm he} = -(\rho_{\rm eh})^*, \quad \rho'_{\rm eh} = -(\rho_{\rm he})^*, \tag{52}$$

which follow from quasiparticle conservation or from the explicit solutions obtained above, and expanding $k_x(\varepsilon) \approx k(0) + \varepsilon/\hbar v_x$ plus terms of order ε^2 that are neglected in the Andreev approximation, one arrives at a nonlinear differential equation for $r^{\rm eff}_{\rm he}(L)$,

$$\frac{dr^{\rm eff}_{\rm he}}{dL} = \frac{2i\varepsilon}{\hbar v_x}r^{\rm eff}_{\rm he} + \rho_{\rm he} - \rho^*_{\rm he}\left(r^{\rm eff}_{\rm he}\right)^2. \tag{53}$$

Solving this equation with the boundary condition $r^{\rm eff}_{\rm he}(0) = 0$ gives

$$r^{\rm eff}_{\rm he}(L) = \frac{\rho_{\rm he}\sin Q_{\rm he}L}{Q_{\rm he}\cos Q_{\rm he}L - i(\varepsilon/\hbar v_x)\sin Q_{\rm he}L}, \tag{54}$$

and similarly,

$$r^{\rm eff}_{\rm eh}(L) = \frac{\rho_{\rm eh}\sin Q_{\rm eh}L}{Q_{\rm eh}\cos Q_{\rm eh}L + i(\varepsilon/\hbar v_x)\sin Q_{\rm eh}L}, \tag{55}$$

where we abbreviated

$$\begin{aligned}Q_{\rm he} &= \sqrt{(\varepsilon/\hbar v_x)^2 - |\rho_{\rm he}|^2},\\ Q_{\rm eh} &= \sqrt{(\varepsilon/\hbar v_x)^2 - |\rho_{\rm eh}|^2}.\end{aligned} \tag{56}$$

Upon taking the expression for $r^{\rm eff}_{\rm he}(L)$ to first order in L, one verifies that one reproduces the starting point $r^{\rm eff}_{\rm he}(\delta L) = \rho_{\rm he}\delta L$ of the previous section. Upon taking $r^{\rm eff}_{\rm he}(L)$ to first order in $\rho_{\rm he}$, one finds

$$r^{\rm eff}_{\rm he}(L) = \rho_{\rm he}\int_0^L dx e^{2i\varepsilon x/\hbar v_x}, \tag{57}$$

which one obtains by applying first-order perturbation theory to the entire superconducting contact of length L at once.[18] Equation (57) represents the effect of a single Andreev reflection at the HS interface, with the phase factor accounting for the relative phase shift between the electron and the Andreev reflected hole for an Andreev reflection taking place at position x. One checks for consistency that $r^{\rm eff}_{\rm he}(\delta L)/\delta L$ turns into Eq. (47) in the limit $\delta L \to 0$.

The relevant limit for the lateral contact of Fig. 1(b) is the limit $L \to \infty$. In this limit, the energy dependence of $r^{\rm eff}_{\rm eh}$ through the energy dependence of $\rho_{\rm he}$ can be neglected in comparison to the explicit energy dependence in Eq. (54), so that one may approximate $\rho_{\rm he}(\mathbf{k}_\perp,\varepsilon)$ by $\rho_{\rm he}(\mathbf{k}_\perp,0)$ in Eq. (54). Defining

$$\begin{aligned}\varepsilon_0(\mathbf{k}_\perp) &= \hbar v_x|\rho_{\rm he}(\mathbf{k}_\perp,0)|\\ &= \frac{\hbar v_z}{2d}|r_{\rm he}(\mathbf{k}_\parallel,0)|,\end{aligned} \tag{58}$$

one then finds that

$$r_{\rm he}^{\rm eff}(\mathbf{k}_\perp,\varepsilon) = \frac{\rho_{\rm he}(\mathbf{k}_\perp,0)}{|\rho_{\rm he}(\mathbf{k}_\perp,0)|} e^{i\arcsin(\varepsilon/\varepsilon_0(\mathbf{k}_\perp))} = \frac{r_{\rm he}(\mathbf{k}_\parallel,0)}{|r_{\rm he}(\mathbf{k}_\parallel,0)|} e^{i\arcsin(\varepsilon/\varepsilon_0(\mathbf{k}_\perp))}, \quad (59)$$

if $\varepsilon < \varepsilon_0(\mathbf{k}_\perp)$. Hence, as long as $\varepsilon < \varepsilon_0(\mathbf{k}_\perp)$, $|r_{\rm he}^{\rm eff}| = 1$ such that a lateral contact serves as an "ideal" contact between a superconductor and a half metal, allowing perfect spin-flip Andreev reflection back into the half metal. For $\varepsilon > \varepsilon_0(\mathbf{k}_\perp)$, $r_{\rm he}(\mathbf{k}_\perp,\varepsilon)$ is an oscillating function of the contact size L, whereas the magnitude of the Andreev reflection amplitude is a decreasing function of energy,

$$\left|r_{\rm he}^{\rm eff}(\mathbf{k}_\perp,\varepsilon)\right|^2 = \frac{\sin^2(Q_{\rm he}L)}{(\varepsilon/\varepsilon_0(\mathbf{k}_\perp))^2 - \cos^2(Q_{\rm he}L)} \approx 1 - \sqrt{1-(\varepsilon_0(\mathbf{k}_\perp)/\varepsilon)^2} \quad \text{if } L\to\infty, \quad (60)$$

where the last line is obtained by averaging L over a period $0 < Q_{\rm he}L < 2\pi$ and is proportional to the envelope of $|r_{\rm he}^{\rm eff}(\varepsilon)|^2$. The energy $\varepsilon_0(\mathbf{k}_\perp)$ separating the regions of complete and partial Andreev reflection can be interpreted as a mode-dependent proximity-induced "minigap" in the half-metallic film.

An analogous calculation including multiple Andreev reflections can be done for the transmission through the contact. For electrons and holes incoming from the left we find the transmission amplitudes

$$t_{\rm ee}^{\rm eff}(\mathbf{k}_\perp,\varepsilon) = \frac{Q_{\rm he}e^{ik_x(0)L}}{Q_{\rm he}\cos Q_{\rm he}L - i(\varepsilon/\hbar v_x)\sin Q_{\rm he}L}, \quad (61)$$

$$t_{\rm hh}^{\rm eff}(\mathbf{k}_\perp,\varepsilon) = \frac{Q_{\rm eh}e^{-ik_x(0)L}}{Q_{\rm eh}\cos Q_{\rm eh}L - i(\varepsilon/\hbar v_x)\sin Q_{\rm eh}L}. \quad (62)$$

The amplitudes for particles incoming from the right are related to Eqs. (61) and (62) by $t_{\rm ee}^{\prime\rm eff} = e^{i2k_x(0)L}t_{\rm hh}^{\rm eff}$ and $t_{\rm hh}^{\prime,\rm eff} = e^{-i2k_x(0)L}t_{\rm ee}^{\rm eff}$. For a long contact, $|\rho_{\rm he}(\mathbf{k}_\perp,\varepsilon)|L \gg 1$ and $\varepsilon < \varepsilon_0(\mathbf{k}_\perp)$ the transmission amplitudes can be approximated as

$$t_{\rm ee}^{\rm eff}(\mathbf{k}_\perp,\varepsilon) \approx 2e^{ik_x(0)L}e^{-q_{\rm he}L}e^{i\arcsin(\varepsilon/\varepsilon_0(\mathbf{k}_\perp))}, \quad (63)$$

with $q_{\rm he} = iQ_{\rm he}$. Thus, $t_{\rm ee}$, $t_{\rm hh}$ become exponentially suppressed consistent with a fully developed proximity effect.

V. APPLICATIONS: SUBGAP CONDUCTANCE AND JOSEPHSON CURRENT

The effective Andreev reflection amplitude $r_{\rm he}^{\rm eff}$ can be used for a calculation of the subgap conductance G and the Josephson current I in a lateral HS or SHS junction in the same way as the Andreev reflection amplitude $r_{\rm he}$ is used in the case of a serial junction.

A. Subgap conductance

In the limit of a long ballistic contact and at the Fermi level $\varepsilon = 0$, the effective Andreev reflection amplitude of Eq. (59) has modulus 1 for all transverse channels (labeled by the integer n and the wave number k_y). Hence the zero bias conductance $G(0)$ is

$$G(0) = G_{\rm m} = \frac{2e^2}{h}N, \quad (64)$$

where

$$N = \frac{k_{\rm H,F}^2 W_y d}{4\pi}, \quad (65)$$

is the number of propagating modes at the Fermi level in the half metal.

Upon increasing V, the Andreev reflection probabilities and hence the conductance G decrease. The precise functional form of this decrease depends on the details of the spin-orbit coupling. For voltages much larger than the induced "minigap" in the half metal, but still much smaller than Δ_0 (i.e., $\hbar v_{\rm F,H}|r_{\rm he}|/2d \ll eV \ll \Delta_0$) we may take $|r_{\rm he}^{\rm eff}(\mathbf{k}_\perp,\varepsilon)|^2$ from Eq. (60) and find

$$G(V) = \frac{e^2}{h}\frac{N\langle\tau^2\rangle_\theta}{128}\left(\frac{\hbar}{eVd}\right)^2 \times \left[2\Omega_{1,x}^2 + \Omega_{1,y}^2 + 2\Omega_{2,x}^2 + \Omega_{2,y}^2\right]. \quad (66)$$

This decay of the subgap conductance with the applied voltage is a marked difference with the case of the serial geometry, for which G is an increasing function of V.

B. Josephson current

The expression for the Josephson current I in a lateral SHS junction can be obtained from Eq. (32) upon setting $r_{\rm ee} = r_{\rm hh} = 0$ and upon replacing $r_{\rm he}$ and $r_{\rm eh}$ by $r_{\rm he}^{\rm eff}$ and $r_{\rm eh}^{\rm eff}$, respectively,

$$I = -\frac{4ek_{\rm B}T}{\hbar}\frac{W_y d}{4\pi^2}{\rm Re}\,\frac{d}{d\phi}\sum_{n=0}^{\infty}\int_{k_\perp<k_{\rm F,H}} d\mathbf{k}_\perp \times \ln\left[1 - r_{\rm he}^{\rm eff}(\mathbf{k}_\perp,i\omega_n)r_{\rm eh}^{\rm eff}(\mathbf{k}_\perp,i\omega_n)'e^{-2\omega_n L_{\rm j}/v_x}\right], \quad (67)$$

where $L_{\rm j}$ is the junction length, see Fig. 2(b), $r_{\rm he}^{\rm eff}(\mathbf{k}_\perp,\varepsilon)$ is the effective electron-to-hole Andreev amplitude of the right superconducting contact for quasiparticles incident from the left, and $r_{\rm eh}^{\rm eff}(\mathbf{k}_\perp,\varepsilon)'$ the effective hole-to-electron Andreev amplitude of the left superconducting contact for quasiparticles incident from the right. We have set the phase of the superconducting order parameter for the right superconductor equal to zero. Upon setting $\varepsilon = i\omega_n$, the effective Andreev reflection amplitudes $r_{\rm he}^{\rm eff}(\mathbf{k}_\perp,\varepsilon)$ and $r_{\rm eh}^{\rm eff}(\mathbf{k}_\perp,\varepsilon)'$ have a well-defined limit for the contact size $L\to\infty$, which is given by Eq. (59) for all ω_n.

We first consider the limit when the minigap $\varepsilon_0 \gg E_{\rm Th}$ is much larger than the Thouless energy $E_{\rm Th} = \hbar v_z/L_{\rm j}$ of the junction (long-junction limit). For high temperatures $k_{\rm B}TL_{\rm j}/\hbar v_{\rm F} \gg 1$, one finds

$$eI = -8\sqrt{2\pi}G_{\rm m}k_{\rm B}Te^{-\frac{2\pi k_{\rm B}TL_{\rm j}}{\hbar v_{\rm F,H}}}\left(\frac{\hbar v_{\rm F,H}}{2\pi k_{\rm B}TL_{\rm j}}\right)^{\frac{3}{2}}\sin\phi. \quad (68)$$

This expression for I has the same sinusoidal phase dependence and exponential junction length dependence as in the serial geometry, but in the lateral contact geometry I is proportional to the much larger conductance $G_{\rm m}$, Eq. (64),

instead of Eq. (30). In the limit of zero temperature, the Josephson current is given by

$$I = \frac{2e}{3}\frac{N v_{\mathrm{F,H}}}{L_{\mathrm{j}}}\phi, \quad -\pi < \phi < \pi, \tag{69}$$

and $I(\phi + 2\pi) = I(\phi)$. Equation (69) is the known form of a supercurrent if the superconductor and the normal junction material are strongly coupled and the junction is disorder-free.[54] The phase dependence is sectionally linear (sawtooth-like) and the critical current decreases with the length L_{j} of the junction.

In the opposite limit of a short junction ($\varepsilon_0 \ll E_{\mathrm{Th}}$), we distinguish three temperature regimes. For very high temperatures $k_{\mathrm{B}}T \gg E_{\mathrm{Th}} = \hbar v_{\mathrm{F,H}}/L_{\mathrm{j}}$, one obtains a sinusoidal phase dependence of the Josephson current

$$I = \frac{3eN\langle\tau^2\rangle_\theta}{8\pi^2\hbar d^2 k_{\mathrm{B}}T}\left(\frac{E_{\mathrm{Th}}}{2\pi k_{\mathrm{B}}T}\right)^2 \times \left(\Omega_{1,x}^2 + \Omega_{2,x}^2\right) e^{-\frac{2\pi k_{\mathrm{B}}T}{E_{\mathrm{Th}}}} \sin\phi. \tag{70}$$

For intermediate temperatures, $\varepsilon_0 \ll k_{\mathrm{B}}T \ll E_{\mathrm{Th}}$, one finds

$$I = \frac{e\hbar N\langle\tau^2\rangle_\theta}{512\, d^2 k_{\mathrm{B}}T}\left(2\Omega_{1,x}^2 + \Omega_{1,y}^2 + 2\Omega_{2,x}^2 + \Omega_{2,y}^2\right)\sin\phi. \tag{71}$$

For $T = 0$, the trace over transverse modes could not be performed in closed form. However, the dependence on phase difference ϕ can be found. One obtains

$$I = \frac{e}{4d}\mathrm{Tr}\{v_z|r_{\mathrm{he}}|\}\sin\frac{\phi}{2}, \quad -\pi < \phi < \pi, \tag{72}$$

and $I(\phi + 2\pi) = I(\phi)$. The dependence $I \propto \sin(\phi/2)$ of the zero-temperature Josephson current is reminiscent of the "fractional Josephson effect," characteristic of Josephson junctions that have Majorana bound states at the superconductor interfaces[39,55] (see also the next section).

VI. MAJORANA STATES

Majorana bound states have been proposed as an elementary building block of a topological quantum computer since they are an example of an excitation with non-Abelian statistics.[46] Majorana bound states exist as the fundamental excitations of a candidate state for the $\nu = 5/2$ quantum Hall effect,[56,57] in vortices in superconductors with a spinless p-wave pairing symmetry,[57–60] or in vortices of s-wave superconductors in contact with a topological insulator[61–63] or a standard 2D electron gas in a large magnetic field and with strong spin-orbit coupling.[40]

Very recently, it was suggested that Majorana bound states can be found at the ends of semiconducting quantum wires with strong spin-orbit coupling and a strong magnetic field, in contact with an s-wave superconductor.[42,43,45] In these proposals, the role of the magnetic field is to create a gap for spin excitations, so that the wires become effectively half metallic. We now show that Majorana bound states also occur in the system considered here: a half-metallic quantum wire in contact with a superconductor with spin-orbit coupling. This enables us to make contact between the (experimentally observed) triplet proximity effect and the, so far, purely theoretical search for avenues to topological quantum computation. Our approach has the additional benefit of providing a fully microscopic description of the p-wave proximity state, in contrast to the existing studies of this effect in semiconducting wires with strong spin-orbit coupling, which rely on an effective description using an induced pairing potential in the semiconducting wire.[42,43]

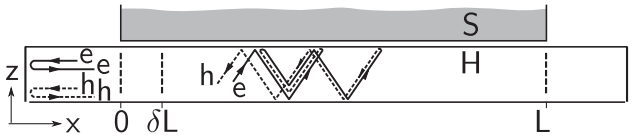

FIG. 3. A lateral contact between a half-metallic film or wire and a superconductor. The contact has length L, with a segment of length δL singled out. The main text describes how the effective Andreev reflection of the entire lateral contact is calculated, starting from the effective Andreev reflection amplitudes $\rho_{\mathrm{he}}\delta L$ and $\rho_{\mathrm{eh}}\delta L$ of the segment of length δL. As discussed in Sec. VI, inserting a normally reflecting boundary at the left end of the H film or wire gives rise to a Majorana bound state.

First, we show that a Majorana state exists at the end of a ballistic half-infinite half-metallic quantum wire laterally coupled to a superconductor. We consider the geometry shown in Fig. 3. The difference with the calculation of Sec. V is that here the half metal is a wire, not a film. We therefore have to use hard-wall boundary conditions in the y direction, not periodic boundary conditions as in Sec. V. With hard-wall boundary conditions, the Andreev reflection amplitudes ρ_{he} and ρ_{eh} per unit length have to be replaced by amplitudes $\tilde{\rho}_{\mathrm{he}}$ and $\tilde{\rho}_{\mathrm{eh}}$, which are defined as

$$\tilde{\rho}_{\mathrm{he}}(k_y,k_z,\varepsilon) = \tfrac{1}{2}[\rho_{\mathrm{he}}(k_y,k_z,\varepsilon) + \rho_{\mathrm{he}}(-k_y,k_z,\varepsilon)], \tag{73}$$

$$\tilde{\rho}_{\mathrm{eh}}(k_y,k_z,\varepsilon) = \tfrac{1}{2}[\rho_{\mathrm{eh}}(k_y,k_z,\varepsilon) + \rho_{\mathrm{eh}}(-k_y,k_z,\varepsilon)]. \tag{74}$$

Since ρ_{he} and ρ_{eh} are odd in k_y, the components of the SOI coupling to k_y drop out. Apart from the replacement $\rho_{\mathrm{he}} \to \tilde{\rho}_{\mathrm{he}}$ and $\rho_{\mathrm{eh}} \to \tilde{\rho}_{\mathrm{eh}}$, the results of Sec. IV continue to hold for the present case.

At the left end of the half-metallic wire, quasiparticles undergo normal reflection with amplitude $s_{\mathrm{H}}(\varepsilon)$ and $s_{\mathrm{H}}(-\varepsilon)^*$ for electron-like and hole-like quasiparticles, respectively. With the Andreev reflection amplitudes of Eq. (59) we then find a nondegenerate bound state at $\varepsilon = 0$ with (unnormalized) wave function

$$\Phi(\mathbf{r}) = i\left[r_{\mathrm{he}}^{\mathrm{eff}}\right]^{-\frac{1}{2}}[s_{\mathrm{H}}(0)\Phi_{\mathrm{e},\mathbf{k}_\perp,+}(\mathbf{r}) + \Phi_{\mathrm{e},\mathbf{k}_\perp,-}(\mathbf{r})] + i\left[r_{\mathrm{he}}^{\mathrm{eff}}\right]^{\frac{1}{2}}[\Phi_{\mathrm{h},\mathbf{k}_\perp,-}(\mathbf{r}) + s_{\mathrm{H}}(0)^*\Phi_{\mathrm{h},\mathbf{k}_\perp,+}(\mathbf{r})], \tag{75}$$

where the scattering states $\Phi_{\mathrm{e},\mathbf{k}_\perp,\pm}$ and $\Phi_{\mathrm{h},\mathbf{k}_\perp,\pm}$ are obtained from those given in Eqs. (40) and (41), but with the replacement $e^{ik_y y} \to \sin(k_y y)$ because of the hard-wall boundary conditions. The distance to the next bound states is of the order of the minigap ε_0 or the level spacing in the normal segment extending from the superconductor, whichever is smaller.

The bound state (75) is identified as a Majorana bound state because it is invariant under electron-hole conjugation (i.e., $\tau_1\Phi^* = \Phi$ where τ_1 is the first Pauli matrix in electron-hole

space). Alternatively, with $\hat{\psi}^\dagger_{\uparrow,\downarrow}, \hat{\psi}_{\uparrow,\downarrow}$ being electron and hole creation operators, Φ corresponds to the field operator

$$\gamma = \int dx [u_\uparrow(\mathbf{x})\hat{\psi}_\uparrow(\mathbf{x}) + v_\uparrow(\mathbf{x})\hat{\psi}^\dagger_\uparrow(\mathbf{x})], \tag{76}$$

with $u_\uparrow = \Phi_1$ and $v_\uparrow = \Phi_3$ given by the electron and hole spin-up component of Φ, respectively. This operator satisfies the condition

$$\gamma = \gamma^\dagger, \tag{77}$$

which is the defining characteristic of a Majorana state. Being a Majorana bound state, Φ is stable against perturbations because, by particle-hole symmetry, a perturbation that moves Φ to some finite energy $\varepsilon \neq 0$ must generate a pair of states at $\pm\varepsilon$. Since Φ is a single state this is not possible.

We note that there is one Majorana mode per transverse mode in the half-metallic wire. Disorder, which is not included here, will lead to interactions between these modes, which will cause Majorana modes to pairwise combine into standard fermionic excitations. If the number of transverse modes is odd, a single Majorana mode is guaranteed to remain present at the end of the half-metallic wire.[44]

If the half-metallic quantum wire has a finite length L, the Majorana bound states at the two ends will interact so that the excitation acquires a finite energy, exponentially small in the length of the wire. This finite excitation energy can be calculated from the full scattering matrix $\mathcal{S}(\varepsilon)$ of the lateral HS contact, calculated in Sec. IV, and the reflection amplitudes $s_{\rm H}(\varepsilon)$ and $s'_{\rm H}(\varepsilon)$ at the left and right ends of the half-metallic wire. The energy spectrum is found from the condition

$$\det(1 - \mathcal{S}_{\rm H}(\varepsilon)\mathcal{S}(\varepsilon)) = 0, \tag{78}$$

where

$$\mathcal{S}_{\rm H}(\varepsilon) = \begin{pmatrix} s_{\rm H}(\varepsilon) & 0 & 0 & 0 \\ 0 & s_{\rm H}(-\varepsilon)^* & 0 & 0 \\ 0 & 0 & s'_{\rm H}(\varepsilon) & 0 \\ 0 & 0 & 0 & s'_{\rm H}(-\varepsilon)^* \end{pmatrix},$$

$$\mathcal{S}(\varepsilon) = \begin{pmatrix} 0 & r^{\rm eff}_{\rm eh}(\varepsilon) & t^{\rm eff}_{\rm ee}(\varepsilon) & 0 \\ r^{\rm eff}_{\rm he}(\varepsilon) & 0 & 0 & t^{\rm eff}_{\rm hh}(\varepsilon) \\ t^{\rm eff}_{\rm ee}(\varepsilon) & 0 & 0 & r^{\rm eff}_{\rm eh}(\varepsilon) \\ 0 & t^{\rm eff}_{\rm hh}(\varepsilon) & r^{\rm eff}_{\rm he}(\varepsilon) & 0 \end{pmatrix}.$$

In the limit of a long contact $|\tilde{\rho}_{\rm he}|L \gg 1$, we then find

$$\varepsilon_\pm = \pm 2|\rho_{\rm he}(\varepsilon)|\hbar v_x(\varepsilon) e^{-|\rho_{\rm he}(\varepsilon)|L} |\sin(k_x(\varepsilon)L)||_{\varepsilon=0}, \tag{79}$$

where we have set $s_{\rm H} = s'_{\rm H} = -1$. Thus, the energy splitting decreases exponentially with the contact length [besides accidental degeneracies for integer $k_x(\varepsilon = 0)L/2\pi$].

It is instructive to compare our calculation with the model of a spinless one-dimensional p-wave superconductor,[39] which has been used as a phenomenological model description of the induced superconductivity in a semiconductor wire with a strong magnetic field and spin-orbit coupling.[41,44] This model has the Hamiltonian

$$H = \frac{p^2}{2m}\tau_0 + \Delta' p \tau_1, \tag{80}$$

where τ_0 is the 2×2 unit matrix in electron-hole space and Δ' the effective p-wave superconducting order parameter. Comparing with our calculation, and specializing to a quantum wire with one quantized mode only, for which $k_z = \pi/d$, we identify

$$|\Delta'| = \frac{\pi\hbar\tau(\mathbf{k}_\perp)}{4d^2\left(k^2_{\rm F,S} - k_x^2 - k_y^2\right)} \sqrt{\Omega^2_{1,x} + \Omega^2_{2,x}}, \tag{81}$$

where $\tau(\mathbf{k}_\perp)$ is the transparency of the interface at the relevant (lowest) transverse mode.

VII. DISCUSSION AND CONCLUSION

In this article, we have shown that spin-orbit interaction in a singlet superconductor gives rise to a triplet proximity effect if the superconductor (S) is coupled to a half-metallic ferromagnet (H). We have calculated the conductance of a HS junction and the Josephson current of a SHS junction in both a serial geometry and in a lateral contact geometry. Because of the coherent effect of multiple Andreev reflections, the effective Andreev amplitudes for a lateral contact geometry are significantly enhanced in comparison to those at a serial geometry. In particular, multiple Andreev reflections at the interface between a clean (disorder-free) half-metallic film or wire and a superconductor can lead to a fully developed triplet proximity effect in the half metal, with an Andreev reflection amplitude of unit magnitude.

The results found here have been derived under the assumption of a ballistic system (i.e., without taking into account disorder scattering in the half metal or in the superconductor). For the single-reflection amplitude $r_{\rm he}$ in Sec. II B this does not strongly restrict the validity of the result since the Andreev reflection amplitude is a microscopic property of the interface: $r_{\rm he}$ is determined by matching the eigenstates on length scales of the Fermi wave length in H and S and the wave function decay length in S. If the disorder is weak, such that the mean free path l exceeds these microscopic length scales, $r_{\rm he}$ will be unchanged by the presence of disorder. In this way, the microscopic Andreev reflection amplitudes calculated in Sec. II B may also serve as a starting point for studies of the conductance of a disordered HS junction or the Josephson current in a disordered SHS junctions. (For example, the Josephson current through a disordered or a chaotic Josephson junction can be found by combining the reflection amplitudes of the clean superconductor interface with the normal-state scattering matrix of the junction, see, e.g., Refs. 52 and 53.)

On the other hand, quantities that rely on free (phase-coherent) propagation in H may change qualitatively in the presence of disorder. Specifically, the effective Andreev reflection amplitude $r^{\rm eff}_{\rm he}$ of the lateral contact has been obtained by phase-coherently summing single reflection amplitudes. At the Fermi energy, these multiple Andreev reflections add constructively because the momentum $\mathbf{k}_\parallel$ parallel to the interface is conserved and amplitudes of subsequent reflections

have the same sign. However, scattering from impurities under the contact will lead to a summation over single amplitudes with different incident angles. Since the Andreev reflection amplitudes $r_{\rm he}$ and $r_{\rm eh}$ are odd in $\mathbf{k}_\parallel$, this sum may no longer be constructive. Thus, the result for $r_{\rm he}^{\rm eff}$ is valid for an ideal, disorder-free lateral contact only. Since the reflection properties of a lateral junction saturate if the junction length $L \gtrsim d/|r_{\rm he}|$, where d is the thickness of the half-metallic film or wire, disorder is not expected to significantly alter our results as long as the elastic mean free path $l \gg d/|r_{\rm he}|$. These conditions need not be met in the two existing experiments[13,14] on the triplet proximity effect in superconductor–half-metal heterostructures, which involve the half metal CrO2.

As a particularly timely application of our calculation, we connect the Andreev reflection amplitudes $r_{\rm he}$ and $r_{\rm eh}$ calculated here to the existence of Majorana bound states at the ends of a ballistic half-metallic quantum wire in (lateral) contact to a superconductor with spin-orbit coupling. This proposal for the construction of Majorana bound states is a variation of a recent proposal that such Majorana bound states exist at the ends of a semiconducting wire in contact with a superconductor, where the semiconductor has strong spin-orbit coupling and the system is placed in a large Zeeman field such that the wire becomes effectively half metallic.[42,43] In our construction, the Zeeman field is replaced by the exchange field in the half metal, and the spin-orbit coupling is not located in the wire, but in the superconductor. It thus avoids the necessity of a (fine-tuned) applied magnetic field, which could negatively interfere with the superconducting order.

Note added. Shortly after our manuscript was submitted, a related eprint appeared,[64] in which it is shown that Majorana edge states appear in a 2D half-metal proximity coupled to an s-wave superconductor with spin-orbit coupling.

ACKNOWLEDGMENTS

We thank B. Béri, J. Kupferschmidt, D. Manske, O. Starykh, A. Schnyder, F. von Oppen, and F. Wilken for discussions. This work was supported by the Alexander von Humboldt foundation.

APPENDIX A: PERTURBATION THEORY IN $\hat{H}_{\rm SO}$

An alternative calculation of the Andreev reflection amplitudes $r_{\rm he}$ and $r_{\rm eh}$ makes use of perturbation theory in the spin-orbit interaction $\hat{H}_{\rm SO}$. For this calculation, finite lateral dimensions $W_x \times W_y$ are assumed, with periodic boundary conditions in the x and y directions.

As before, we consider wave functions proportional to $e^{ik_x x+ik_y y}$. In the absence of spin-orbit coupling, there are two linearly independent solutions of the Bogoliubov-de–Gennes equation for each pair k_x,k_y. The first of these is "electron-like," and of the general form

$$\Psi_{\mathbf{e}\mathbf{k}_\parallel}(\mathbf{r}) = \frac{c_{\mathrm{e}\uparrow}e^{ik_z(\varepsilon)z} + c'_{\mathrm{e}\uparrow}e^{-ik_z(\varepsilon)z}}{\sqrt{v_z(\varepsilon)W_xW_y}} \times e^{ik_xx+ik_yy}(1,0,0,0)^{\rm T} + c_{\mathrm{h}\downarrow}e^{ik_xx+ik_yy+\kappa_z(-\varepsilon)z}(0,0,0,1)^{\rm T}, \quad \text{(A1)}$$

for $z < 0$ and

$$\Psi_{\mathbf{e}\mathbf{k}_\parallel}(\mathbf{r}) = d'_\uparrow e^{ik_xx+ik_yy+iq_+z}(1,0,0,e^{-i\phi-i\eta})^{\rm T} + d_\uparrow e^{ik_xx+ik_yy+iq_-z}(1,0,0,e^{-i\phi+i\eta})^{\rm T}, \quad \text{(A2)}$$

for $z > 0$, where

$$q_s = s\sqrt{k_{\rm F,S}^2 - k_x^2 - k_y^2 + 2ism\sqrt{\Delta_0^2-\varepsilon^2}}. \quad \text{(A3)}$$

The boundary conditions (22) with $\Omega_{j,z} = 0$ give four equations for the five coefficients $c_{\mathrm{e},\uparrow}$, $c'_{\mathrm{e},\uparrow}$, $c_{\mathrm{h},\downarrow}$, $d_\uparrow$, and $d'_\uparrow$ so that one coefficient can be chosen freely. Choosing $c_{\mathrm{e},\uparrow} = 1$ one obtains the "retarded scattering state" $\Psi^{\rm R}_{\mathrm{e},\mathbf{k}_\parallel}$, while choosing $c'_{\mathrm{e},\uparrow} = 1$ one obtains the "advanced scattering state" $\Psi^{\rm A}_{\mathrm{e},\mathbf{k}_\parallel}$.

The second scattering state is "hole-like" and has the general form

$$\Psi_{\mathbf{h}\mathbf{k}_\parallel}(\mathbf{r}) = \frac{c_{\mathrm{h}\uparrow}e^{-ik_z(-\varepsilon)z} + c'_{\mathrm{h}\uparrow}e^{ik_z(-\varepsilon)z}}{\sqrt{v_z(-\varepsilon)W_xW_y}} \times e^{ik_xx+ik_yy}(0,0,1,0)^{\rm T} + c_{\mathrm{e}\downarrow}e^{ik_xx+ik_yy+\kappa_z(\varepsilon)z}(0,1,0,0)^{\rm T}, \quad \text{(A4)}$$

for $z < 0$ and

$$\Psi_{\mathbf{h}\mathbf{k}_\parallel}(\mathbf{r}) = d'_\downarrow e^{ik_xx+ik_yy+iq_+z}(0,1,-e^{-i\phi-i\eta},0)^{\rm T} + d_\downarrow e^{ik_xx+ik_yy+iq_-z}(0,1,-e^{-i\phi+i\eta},0)^{\rm T}, \quad \text{(A5)}$$

for $z > 0$. The boundary conditions (22) with $\Omega_{j,z} = 0$ give four equations for the five coefficients $c_{\mathrm{e},\downarrow}$, $c_{\mathrm{h},\uparrow}$, $c'_{\mathrm{h},\uparrow}$, $d_\downarrow$, and $d_{\downarrow'}$ (see Ref. 18 for details). Choosing $c_{\mathrm{e},\uparrow} = 1$ one obtains the "retarded scattering state" $\Psi^{\rm R}_{\mathrm{e},\mathbf{k}_\parallel}$, while choosing $c'_{\mathrm{e},\uparrow} = 1$ one obtains the "advanced scattering state" $\Psi^{\rm A}_{\mathrm{e},\mathbf{k}_\parallel}$.

In the Born approximation, the Andreev reflection amplitudes to first order in the spin-orbit interaction are then found as the matrix element

$$r_{\rm he}(\mathbf{k}_\parallel,\varepsilon) = -i\langle\Psi^{\rm A}_{\mathrm{h},\mathbf{k}_\parallel}|\mathcal{H}_{\rm SO}|\Psi^{\rm R}_{\mathrm{e},\mathbf{k}_\parallel}\rangle, \quad \text{(A6)}$$

$$r_{\rm eh}(\mathbf{k}_\parallel,\varepsilon) = -i\langle\Psi^{\rm A}_{\mathrm{e},\mathbf{k}_\parallel}|\mathcal{H}_{\rm SO}|\Psi^{\rm R}_{\mathrm{h},\mathbf{k}_\parallel}\rangle, \quad \text{(A7)}$$

between retarded and advanced scattering states, where $\mathcal{H}_{\rm SO}$ is given by Eq. (46).

Inserting the explicit expressions for the scattering states into Eqs. (A6) and (A7) then gives the Andreev reflection amplitudes of Eqs. (23) and (24).

Note that only the wave functions in the superconducting region $z > 0$ enter into the calculation of the Andreev reflection amplitudes. The observation that the SOI proportional to $\Omega_{1,z}$ or $\Omega_{2,z}$ does not give rise to Andreev reflection to first order in the SOI then follows from the observation that the matrix elements (A6) and (A7) vanish for arbitrary coefficients $d_\uparrow$, $d'_\uparrow$, $d_\downarrow$, and $d'_\downarrow$ if $\hat{H}_{\rm SO}$ contains $\Omega_{1,z}$ or $\Omega_{2,z}$ only.

APPENDIX B: TRIPLET PAIRINGS IN S

In this Appendix we give the results for the Andreev reflection amplitudes in the presence of finite triplet pairings in S which are linear in momentum. The triplet proximity effect in a half metal in contact with a spin-triplet superconductor was also considered by Linder *et al.*[12] We consider a pairing of the form

$$\Delta_i(\mathbf{p}) = \sum_{j=1}^{3} d_{ij} p_j, \tag{B1}$$

where d_{ij} are the components of the triplet order parameter which is taken as a small correction to the spin singlet s-wave pairing $\Delta_0 e^{i\phi}$ (see Sec. II). In a similar calculation as in the main text we find the Andreev reflection amplitude $r_{\rm he}^{\rm t}$ induced by $\Delta_i(\mathbf{p})$ to first order in $\Delta_i(\mathbf{p})$. The amplitude $r_{\rm he}^{\rm t} = r_{\rm he}^{\rm t,e} + r_{\rm he}^{\rm t,o}$ contains contributions $r_{\rm he}^{\rm t,e}$, $r_{\rm he}^{\rm t,o}$ that are even and odd in momentum, respectively. We find

$$r_{\rm he}^{\rm t,e} = \frac{\varepsilon\tau(\theta)}{2\left(\Delta_0^2 - \varepsilon^2\right)}(d_{13}^* + i d_{23}^*)\sqrt{k_{\rm F,S}^2 - k_{F,H}^2 \sin^2\theta}, \tag{B2}$$

and

$$r_{\rm he}^{\rm t,o} = \sum_{j=1}^{3} k_{\|,j} \frac{i\tau(\theta)}{2}\left[\frac{d_{1j}^* + i d_{2j}^*}{\left(\Delta_0^2 - \varepsilon^2\right)^{\frac{1}{2}}} - \frac{\Delta_0^2}{2}\frac{(d_{1j}^* + i d_{2j}^*) + e^{-2i\phi}(d_{1j} + i d_{2j})}{\left(\Delta_0^2 - \varepsilon^2\right)^{\frac{3}{2}}}\right], \tag{B3}$$

for the electron-to-hole conversion amplitudes and

$$r_{\rm eh}^{\rm t}(\mathbf{k}_\|, \varepsilon) = \left[r_{\rm he}^{\rm t}(-\mathbf{k}_\|, -\varepsilon)\right]^*, \tag{B4}$$

for the opposite process. Triplet pairings can be included in the calculation of the conductance and the Josephson current by the substitution

$$r_{\rm he} \to r_{\rm he} + r_{\rm he}^{\rm t}. \tag{B5}$$

The enhancement due to multiple Andreev reflections found in the second part of the article for the lateral geometry does not rely on the details of $r_{\rm he}$ and is not changed by the presence of the Δ_i. For a detailed discussion of amplitudes that are odd or even in frequency we refer to Ref. 18.

[1] F. S. Bergeret, A. F. Volkov, and K. B. Efetov, Rev. Mod. Phys. **77**, 1321 (2005).
[2] A. I. Buzdin, Rev. Mod. Phys. **77**, 935 (2005).
[3] A. Andreev, Sov. Phys. JETP **19**, 1228 (1964).
[4] F. S. Bergeret, A. F. Volkov, and K. B. Efetov, Phys. Rev. Lett. **86**, 4096 (2001).
[5] A. Kadigrobov, R. I. Shekhter, and M. Jonson, Europhys. Lett. **54**, 394 (2001).
[6] V. T. Petrashov, I. A. Sosnin, I. Cox, A. Parsons, and C. Troadec, Phys. Rev. Lett. **83**, 3281 (1999).
[7] I. Sosnin, H. Cho, V. T. Petrashov, and A. F. Volkov, Phys. Rev. Lett. **96**, 157002 (2006).
[8] V. N. Krivoruchko and V. Y. Tarenkov, Phys. Rev. B **75**, 214508 (2007).
[9] K. A. Yates, W. R. Branford, F. Magnus, Y. Miyoshi, B. Morris, L. F. Cohen, P. M. Sousa, O. Conde, and A. J. Silvestre, Appl. Phys. Lett. **91**, 172504 (2007).
[10] T. S. Khaire, M. A. Khasawneh, W. P. Pratt, and N. O. Birge, Phys. Rev. Lett. **104**, 137002 (2010).
[11] S. Wu and K. V. Samokhin, Phys. Rev. B **80**, 014516 (2009).
[12] J. Linder and A. Sudbø, Phys. Rev. B **76**, 054511 (2007); J. Linder, M. Cuoco, and A. Sudbø, *ibid.* **81**, 174526 (2010).
[13] R. S. Keizer, S. T. B. Goennenwein, T. M. Klapwijk, G. Miao, G. Xiao, and A. Gupta, Nature (London) **439**, 825 (2006).
[14] M. S. Anwar, F. Czeschka, M. Hesselberth, M. Porcu, and J. Aarts, Phys. Rev. B **82**, 100501 (2010).
[15] M. Eschrig and T. Löfwander, Nature Phys. **4**, 138 (2008).
[16] Y. Asano, Y. Tanaka, and A. A. Golubov, Phys. Rev. Lett. **98**, 107002 (2007); Y. Asano, Y. Sawa, Y. Tanaka, and A. A. Golubov, Phys. Rev. B **76**, 224525 (2007).
[17] B. Béri, J. N. Kupferschmidt, C. W. J. Beenakker, and P. W. Brouwer, Phys. Rev. B **79**, 024517 (2009).
[18] J. N. Kupferschmidt and P. W. Brouwer, Phys. Rev. B **83**, 014512 (2011).
[19] J. N. Kupferschmidt and P. W. Brouwer, Phys. Rev. B **80**, 214537 (2009).
[20] F. Wilken, Diploma thesis, Freie Universität Berlin, 2010.
[21] S. LaShell, B. A. McDougall, and E. Jensen, Phys. Rev. Lett. **77**, 3419 (1996).
[22] E. I. Rashba, Sov. Phys. Solid State **2**, 1109 (1960).
[23] J. Nitta, T. Akazaki, H. Takayanagi, and T. Enoki, Phys. Rev. Lett. **78**, 1335 (1997).
[24] Y. K. Kato, R. C. Myers, A. C. Gossard, and D. D. Awschalom, Nature (London) **427**, 50 (2004).
[25] E. Bauer, G. Hilscher, H. Michor, C. Paul, E. W. Scheidt, A. Gribanov, Y. Seropegin, H. Noël, M. Sigrist, and P. Rogl, Phys. Rev. Lett. **92**, 027003 (2004).
[26] M. Sigrist, D. F. Agterberg, P. A. Frigeri, N. Hayashi, R. P. Kaur, A. Koga, I. Milat, K. Wakabayashi, and Y. Yanase, J. Magn. Magn. Mater. **310**, 536 (2007).
[27] D. F. Agterberg, Physica C **387**, 13 (2003).
[28] K. V. Samokhin, Phys. Rev. B **70**, 104521 (2004).
[29] R. P. Kaur, D. F. Agterberg, and M. Sigrist, Phys. Rev. Lett. **94**, 137002 (2005).
[30] M. Sigrist and K. Ueda, Rev. Mod. Phys. **63**, 239 (1991).
[31] P. A. Frigeri, D. F. Agterberg, A. Koga, and M. Sigrist, Phys. Rev. Lett. **92**, 097001 (2004).
[32] K. D. Nelson, Z. Q. Mao, Y. Maeno, and Y. Liu, Science **306**, 1151 (2004).
[33] C. Iniotakis, N. Hayashi, Y. Sawa, T. Yokoyama, U. May, Y. Tanaka, and M. Sigrist, Phys. Rev. B **76**, 012501 (2007); Y. Tanaka, T. Yokoyama, A. V. Balatsky, and N. Nagaosa, *ibid.* **79**, 060505 (2009).
[34] V. M. Edelstein, J. Phys. C **7**, 1 (1995).
[35] S. Fujimoto, Phys. Rev. B **72**, 024515 (2005).

[36]L. P. Gor'kov and E. I. Rashba, Phys. Rev. Lett. **87**, 037004 (2001).
[37]S. K. Yip, Phys. Rev. B **65**, 144508 (2002).
[38]V. Braude and Y. V. Nazarov, Phys. Rev. Lett. **98**, 077003 (2007).
[39]A. Y. Kitaev, e-print arXiv:cond-mat/0010440.
[40]J. D. Sau, R. M. Lutchyn, S. Tewari, and S. Das Sarma, Phys. Rev. Lett. **104**, 040502 (2010).
[41]P. A. Lee, e-print arXiv:0907.2681.
[42]R. M. Lutchyn, J. D. Sau, and S. Das Sarma, Phys. Rev. Lett. **105**, 077001 (2010).
[43]Y. Oreg, G. Refael, and F. von Oppen, Phys. Rev. Lett. **105**, 177002 (2010).
[44]A. C. Potter and P. A. Lee, Phys. Rev. Lett. **105**, 227003 (2010).
[45]J. Alicea, Y. Oreg, G. Refael, F. von Oppen, and M. P. A. Fisher, Nature Phys. (2011), doi:10.1038/nphys1915.
[46]C. Nayak, S. H. Simon, A. Stern, M. Freedman, and S. Das Sarma, Rev. Mod. Phys. **80**, 1083 (2008).
[47]K. K. Likharev, Rev. Mod. Phys. **51**, 101 (1979).
[48]Note that the SOI is position dependent and the operator ordering of z and p_z in $\hat{H}05EH_{\rm SO}$ has to be defined. Only for linear-in-momentum SOI's is the ordering uniquely determined by the hermiticity of the Hamiltonian. SOI's with higher orders in p_z require a microscopic derivation of an effective-mass Hamiltonian for an atomically sharp interface, see, for example, M. G. Burt, Phys. Rev. B **50**, 7518 (1994).
[49]M. Tinkham, *Introduction to Superconductivity* (Dover Publications, New York, 2004).
[50]G. E. Blonder, M. Tinkham, and T. M. Klapwijk, Phys. Rev. B **25**, 4515 (1982).
[51]Y. Takane and H. Ebisawa, J. Phys. Soc. Jpn. **61**, 1685 (1992).
[52]C. W. J. Beenakker, Phys. Rev. Lett. **67**, 3836 (1991).
[53]P. Brouwer and C. Beenakker, Chaos Solitons Fractals **8**, 1249 (1997).
[54]C. Ishii, Prog. Theor. Phys. **44**, 1525 (1970).
[55]L. Fu and C. L. Kane, Phys. Rev. B **79**, 161408 (2009).
[56]G. Moore and N. Read, Nucl. Phys. B **360**, 362 (1991).
[57]N. Read and D. Green, Phys. Rev. B **61**, 10267 (2000).
[58]D. A. Ivanov, Phys. Rev. Lett. **86**, 268 (2001).
[59]A. Stern, F. von Oppen, and E. Mariani, Phys. Rev. B **70**, 205338 (2004).
[60]M. Stone and S.-B. Chung, Phys. Rev. B **73**, 014505 (2006).
[61]L. Fu and C. L. Kane, Phys. Rev. Lett. **100**, 096407 (2008).
[62]A. R. Akhmerov, J. Nilsson, and C. W. J. Beenakker, Phys. Rev. Lett. **102**, 216404 (2009).
[63]Y. Tanaka, T. Yokoyama, and N. Nagaosa, Phys. Rev. Lett. **103**, 107002 (2009).
[64]S. B. Chung, H.-J. Zhang, X.-L. Qi, and S. C. Zhang, e-print arXiv:1011.6422.